

## Clustering Dynamics of the Metal–Benzene Sandwich Complex: The Role of Microscopic Structure of the Solute In the Bis( $\eta^6$ -benzene)chromium $\cdot$ Ar $_n$ Clusters ( $n = 1–15$ )

Kyo-Won Choi, Sunyoung Choi, Doo-Sik Ahn, Songhee Han, Tae Yeon Kang, Sun Jong Baek, and Sang Kyu Kim\*

Department of Chemistry and School of Molecular Science (BK21), KAIST, Daejeon (301–750), Republic of Korea

Received: May 24, 2008; Revised Manuscript Received: June 25, 2008

Ar clustering dynamics around the metal-benzene sandwich complex, bis( $\eta^6$ -benzene)chromium: Cr(Bz) $_2$ , is found to occur in two distinct regimes. The shift of the ionization potential (IP) upon the addition of Ar is measured to be 151 cm $^{-1}$ , and it is constant until the number of Ar solvents ( $n$ ) becomes 6. The IP shift per Ar is found to be suddenly decreased to 82 cm $^{-1}$  for the clusters of  $n = 7–12$ . The cluster distribution indicates that the  $n = 6$  cluster is most populated in the molecular beam. These experimental findings with the aid of ab initio calculation indicate that the first six Ar solvent molecules are attached to top and bottom of Cr(Bz) $_2$  to give the robust structure for the Cr(Bz) $_2$ –Ar $_6$  cluster whereas the next six Ar molecules are gathered on the side of the solute core to give the highly symmetric structure of the Cr(Bz) $_2$ –Ar $_{12}$  cluster.

Cluster chemistry has been both intensively and extensively studied as the relation of the structure and chemical reactivity in the presence of solute–solvent interactions can be unambiguously investigated at the atomic level. Unlike the hydrogen-bonded cluster of which the geometrical layout is determined by the local charge distribution of the solute core, the structures of van der Waals clusters are often considered to be less sensitive to the microscopic structure of the solute because the dispersive force is usually not oriented in a particular direction with respect to the specific nuclear layout.<sup>1,2</sup> Accordingly, the effect of the microscopic solute-structure on the whole geometrical layout of the associated van der Waals cluster has been little studied to date. In this communication, we have found that the metal–benzene sandwich complex, because of its highly symmetric structure, plays an important role in the determination of the cluster structure. The understanding of noncovalent interactions in the close proximity of the organometallic compound might be quite useful for the understanding of the catalytic process at the molecular level.<sup>3</sup> Additionally, because the organometallic compound in porous composites is currently being considered as a potential container for the hydrogen storage,<sup>4,5</sup> van der Waals interaction in the vicinity of the metal–organic sandwich complex could be quite informative in this regard.

Here, we have investigated the Ar clustering dynamics of the metal-benzene sandwich complex, bis( $\eta^6$ -benzene)chromium or Cr(Bz) $_2$ . Bis( $\eta^6$ -benzene)chromium was purchased from Aldrich (97%) and used without further purification. The sample was heated at 110 °C, mixed with the Ar carrier gas, expanded into vacuum chamber through a 0.8 mm diameter nozzle orifice (General Valve series 9) with a backing pressure of 1.5 atm. The resultant supersonic jet was then skimmed through a 1 mm

diameter skimmer (Precision Instrument) before it was collinearly overlapped with the UV laser pulse. The background pressure of  $\sim 10^{-7}$  Torr was maintained when the nozzle was operated with a 10 Hz repetition. A tunable laser pulse (1–2 mJ/pulse,  $\Delta t \sim 5$  ns) in the 220–228 nm range was generated by the frequency doubling of the output of a dye laser (Lambda Physik, Scanmate 2) pumped by the third harmonic output of a Nd:YAG laser (Continuum, Precision II) through a BBO crystal placed on a homemade autotracker. The generated ions were extracted after a certain delay time, accelerated, drafted along the time-of-flight axis and detected by dual multichannel plates. The signals were digitized by an oscilloscope (LeCroy, LT584M) and stored in a personal computer. Photoionization efficiency spectrum of each cluster was obtained by monitoring the corresponding cluster ion signal as a function of the excitation laser wavelength. For mass-analyzed threshold ionization (MATI) spectra, the pulsed field ionization method was employed to detect the long-lived high- $n, l$  Rydberg states generated by the UV laser excitation.

Photoionization efficiency (PIE) spectrum of each mass-selected Cr(Bz) $_2$ –Ar $_n$  cluster has been taken using the delayed pulsed-field ionization method for  $n = 1–15$ , Figure 1. The onset found at the sharply rising edge of the PIE signal corresponds to the adiabatic ionization potential (IP), as clearly demonstrated in the comparison of mass-analyzed threshold ionization (MATI) and PIE spectra for  $n = 0, 1$  and 2, Figure 1. The sharp rise of PIE at the ionization threshold strongly indicates that the 0–0 $^+$  origin is the strongest band, and thus the cluster structure remains almost same upon the ionization. And also, as shown in the PIE and MATI spectra of the Cr(Bz) $_2$ –Ar $_2$  cluster in Figure 1, the sharp rise of PIE indicates that there is only a single structural isomer in the beam. The IP shows the red shift as the cluster size increases. The IP of the bare Cr(Bz) $_2$  is 5.4665 eV $^{6-9}$  whereas that of the Cr(Bz) $_2$ –Ar

\* Corresponding author; Fax: +82-42-869-2810; E-mail: sangkyukim@kaist.ac.kr

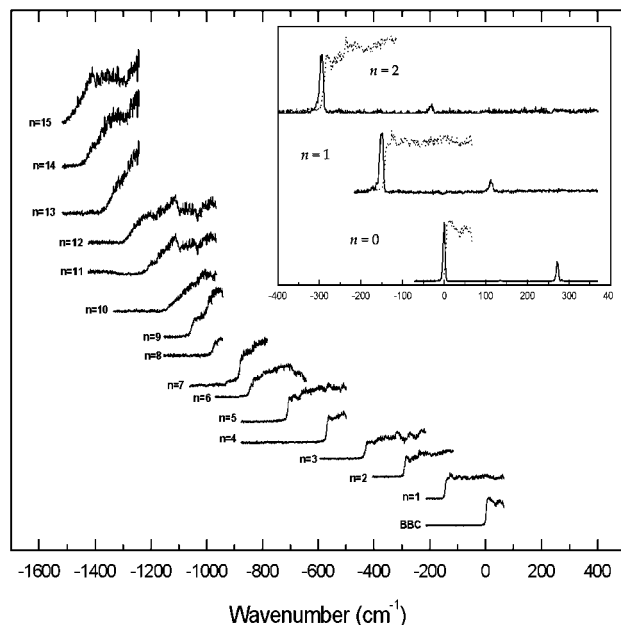


**Figure 1.** Photoionization efficiency spectra of the  $\text{Cr}(\text{Bz})_2\text{-Ar}_n$  clusters. In the inset, MATI spectra of  $\text{Cr}(\text{Bz})_2$ ,  $\text{Cr}(\text{Bz})_2\text{-Ar}$ , and  $\text{Cr}(\text{Bz})_2\text{-Ar}_2$  are shown with corresponding PIE spectra for the comparison. BBC =  $\text{Cr}(\text{Bz})_2$ .

cluster is found to be red-shifted by  $151\text{ cm}^{-1}$  to give the corresponding IP of  $5.4477 \pm 0.0006\text{ eV}$ .

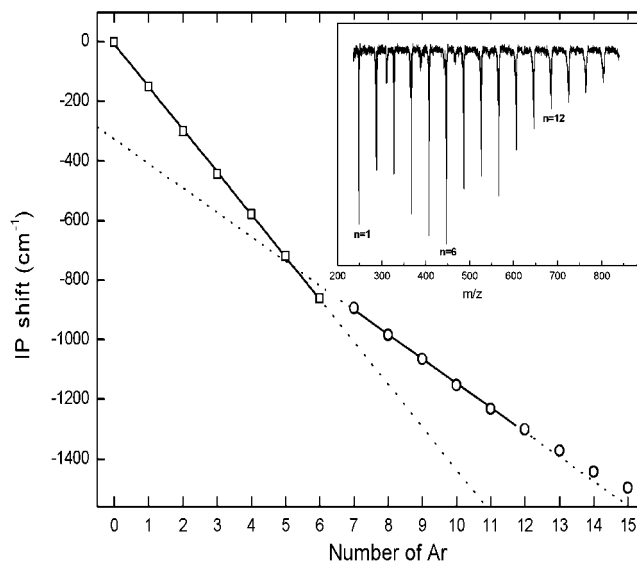
Interestingly, the IP shift of  $151\text{ cm}^{-1}$  upon the single Ar atom clustering is found to be very regular until the number of Ar atoms surrounding  $\text{Cr}(\text{Bz})_2$  becomes 6. The red shift of IP upon clustering indicates that the binding energy of the cluster becomes higher as the cluster is ionized. The relation of the IP shift as a function of the cluster size can be written as follows.

$$\text{IP}(n-1) - \text{IP}(n) = \text{BE}^+(n \rightarrow n-1) - \text{BE}(n \rightarrow n-1) \quad (1)$$

Here,  $n$  is the number of Ar atoms,  $\text{BE}(n \rightarrow n-1)$  is the binding energy of the  $\text{Cr}(\text{Bz})_2\text{-Ar}_n$  cluster with respect to the asymptotic limit of the  $\text{Cr}(\text{Bz})_2\text{-Ar}_{n-1} + \text{Ar}$  dissociation, and  $\text{BE}^+(n \rightarrow n-1)$  is that for the ion. Suppose that the binding energy is proportional to the number of solvent molecules for both neutral and cationic clusters, then  $\text{BE}(n \rightarrow n-1) = n\text{BE}(1 \rightarrow 0)$  and  $\text{BE}^+(n \rightarrow n-1) = n\text{BE}^+(1 \rightarrow 0)$ , giving the following relation.

$$\Delta\text{IP} = \text{IP}(n-1) - \text{IP}(n) = n[\text{BE}^+(1 \rightarrow 0) - \text{BE}(1 \rightarrow 0)] \quad (2)$$

In this case, the IP shift is proportional to  $n$ , and the slope corresponds to the energy difference between binding energy of  $\text{Cr}(\text{Bz})_2\text{-Ar}$  in the neutral ground state and that in the cationic ground state. The straight line shown in Figure 2 from  $n = 0$  to  $n = 6$ , therefore, strongly suggests that the binding energy of the solute-solvent cluster is equally increased as the additional Ar is attached to the solute core until the number of the solvent molecules becomes six. From  $n = 7$ , however, the IP shift is found to be suddenly decreased to  $82\text{ cm}^{-1}$ , indicating that the Ar cluster binding site becomes different and its associated binding energy probably weaker. Interestingly, the IP shift plotted from  $n = 7$  to 12 gives another straight line with a slope of  $82\text{ cm}^{-1}$ . This experimental fact indicates that the clustering site may be equivalent for the seventh to twelfth addition of Ar in terms of its binding energy per Ar. For the clusters larger than  $n = 9$ , instead of sharp rising edges, the PIE spectrum shows the smoothly rising curve at the ionization threshold, suggesting that the Ar solvent becomes less rigid and the intermolecular structural change upon the ionization is severe,

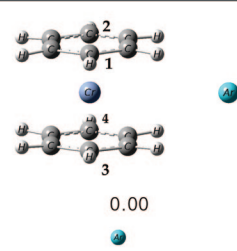
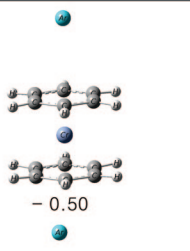
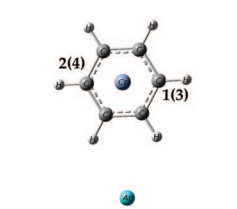
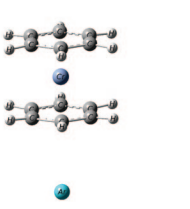
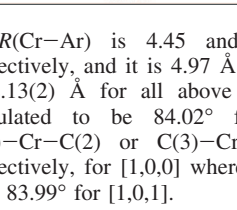


**Figure 2.** IP shift versus the number of Ar in the cluster. The uncertainty of IP is less than the size of the point. Inset: time-of-flight distribution of the clusters showing the maximum intensity at  $n = 6$ . The irregular peak at  $n = 9$  is also noteworthy (see the text).

Figure 1. The present IP trend as a function of the cluster size gives the important insight into the clustering dynamics of  $\text{Cr}(\text{Bz})_2\text{-Ar}_n$ . That is, Ar clustering takes place on the equivalent binding site of  $\text{Cr}(\text{Bz})_2$  until  $n = 6$ , and then another at least six equivalent binding sites of the cluster are occupied for the larger clusters of  $n \geq 7$  with the relatively weaker binding energy. This makes the  $\text{Cr}(\text{Bz})_2\text{-Ar}_6$  cluster ( $n = 6$ ) unique in terms of the structure and stability. For instance, in the time-of-flight (TOF) spectrum in Figure 2, the relative population of the clusters is peaked at the Ar clustering number of 6. The maximum ion intensity at  $n = 6$  indicates that the  $\text{Cr}(\text{Bz})_2\text{-Ar}_6$  cluster is robust, because otherwise the excitation of the large clusters much above the dissociation threshold should result in the efficient fragmentation leading to the relatively larger population of the small clusters. No such a cluster distribution had been observed for the much studied benzene-Ar clusters.<sup>10-12</sup> It is noteworthy that the population of the  $n = 9$  cluster is also irregularly peaked in the cluster distribution. This observation, with the fact that the  $\text{Cr}(\text{Bz})_2\text{-Ar}_9$  cluster is the largest cluster showing the sharp rising edge in the PIE spectrum, leads us to conclude that there may be another robust structure at  $n = 9$ .

The  $\text{Cr}(\text{Bz})_2$  molecule belongs to  $D_{6h}$ , and thus the six equivalent binding sites for Ar solvent molecules are quite well conceivable. Considering the symmetric nature of the  $\text{Cr}(\text{Bz})_2$  molecule, there are three plausible structures for the  $\text{Cr}(\text{Bz})_2\text{-Ar}_6$  cluster. The first structure is the one in which six Ar molecules are directed to the center Cr atom from the six equivalent side positions between two benzene moieties. Alternatively, all six Ar molecules may attach to one side of benzene plane of  $\text{Cr}(\text{Bz})_2$  or three Ar molecules could be noncovalently attached to each benzene plane of the solute core. These three possible structural isomers can be designated as [0,6,0], [6,0,0], or [3,0,3] where  $n_1$ ,  $n_2$ , and  $n_3$  in  $[n_1, n_2, n_3]$  represent the number of Ar solvent molecules attached to the top, side, and bottom of  $\text{Cr}(\text{Bz})_2$ , respectively. Considering the steric hindrance and entropy factors, the most crowded [6,0,0] structure seems to be least likely.<sup>10-12</sup> Therefore, the  $\text{Cr}(\text{Bz})_2\text{-Ar}_6$  cluster may adopt either the [0,6,0] or [3,0,3] structure. The origin of the cluster binding force is mainly the dispersive interaction, but the induced dipole interaction could

**TABLE 1: Relative Energies (kcal/mol) of the Cr(Bz)<sub>2</sub>-Ar<sub>n</sub> Clusters Predicted by MP2<sup>a</sup>**

[0,n <sub>2</sub> ,0]	[n <sub>1</sub> ,0,n <sub>3</sub> ]
	
	
	

<sup>a</sup>  $R(\text{Cr}-\text{Ar})$  is 4.45 and 4.50 Å for [0,1,0] and [0,2,0], respectively, and it is 4.97 Å for both [1,0,0] and [1,0,1].  $R(\text{Cr}-\text{C})$  is 2.13(2) Å for all above structures. All C-Cr-C angles are calculated to be 84.02° for both [0,1,0] and [0,2,0]. The C(1)-Cr-C(2) or C(3)-Cr-C(4) angle is 84.08° or 83.92°, respectively, for [1,0,0] whereas these are calculated to be same to give 83.99° for [1,0,1].

also be responsible depending on the charge allocation in the cluster. In the case of the Cr(Bz)<sub>2</sub>-Ar<sub>n</sub> cluster, because of the nature of the metal-to-ligand charge transfer partly occurring even in the ground state, two benzene moieties have partial negative charges whereas the Cr atom has a partial positive charge.<sup>13-15</sup> For instance, a recent study on the energy partitioning analysis of the metal-ligand bond<sup>15</sup> suggests that the Cr-benzene interaction in Cr(Bz)<sub>2</sub> is 38% electrostatic and 62% covalent in nature mainly via the metal-to-ligand  $\delta$  back-donation. Therefore, even though the charge of the whole molecule is neutral, the Cr(Bz)<sub>2</sub> molecule has two internal weak dipoles of which directions are opposite to each other. These weak internal dipoles may contribute to the induced dipole interaction along the longitudinal axis of Cr(Bz)<sub>2</sub>, making the [3,0,3] structure to be the preferred one. Because the deficiency of an electron in the d<sub>z<sup>2</sup></sub> orbital of the cationic state induces the change of the charge distribution along the Br-Cr-Bz axis, the extent of stabilization of the [3,0,3] structure upon ionization is likely to be larger than that of [0,6,0]. This supports the [3,0,3] structure for the Cr(Bz)<sub>2</sub>-Ar<sub>6</sub> cluster because the IP shift upon clustering, which corresponds to the extent of stabilization upon ionization, is expected to be higher for [n<sub>1</sub>,0,n<sub>2</sub>] clusters compared to that for [0,n<sub>3</sub>,0] where n<sub>1</sub>, n<sub>2</sub> ≤ 3 and n<sub>3</sub> ≤ 6.

The MP2 calculation has been carried out for the elucidation of the most stable structure of the clusters using the Gaussian03 electronic structure package.<sup>16</sup> The CRENBL-ECP<sup>17</sup> was used for Cr whereas the 6-31++G(d,p) was used for C and H. The aug-cc-pVTZ basis set was used for Ar. Spin multiplicities are 1 for all atoms. The [1,0,0] structure is predicted to be more stable than the [0,1,0] structure for n = 1 whereas the [1,0,1] structure is favored compared to the [0,2,0] structure for n = 2 by the preliminary MP2 calculation in this work, Table 1. This theoretical result is consistent with the predication based on the

qualitative description of the metal-ligand bond described above. For the cluster of n = 6, it turns out to be nontrivial to explore all possible [3,0,3] local minimum structures among which the geometrical difference could be subtle. Nevertheless, because the experiment clearly indicates that the Ar clustering dynamics around Cr(Bz)<sub>2</sub> occurs in two distinct regimes, it is concluded here that the first six Ar solvent molecules are attached to the top and bottom of Cr(Bz)<sub>2</sub> to give the [3,0,3] structure for the Cr(Bz)<sub>2</sub>-Ar<sub>6</sub> cluster whereas the next six Ar molecules are gathered on the side of the solute core to give the [3,6,3] structure for the Cr(Bz)<sub>2</sub>-Ar<sub>12</sub> cluster. Theoretical calculations for large clusters are quite demanding, and subjected to further investigation. This report demonstrates that the microscopic structure of the solute at the atomic level plays an important role in the clustering dynamics. Clustering dynamics around the metal-organic sandwich complex in general should provide the fundamental framework for the understanding of the solute-solvent interaction in many catalytic reactions and possibly the mechanism of the hydrogen storage around the unique structure of the organometallic compound.

**Acknowledgment.** This work was financially supported by KOSEF (R01-2007-000-10766-0 & M10703000936-07M0300-93610), Echo technopia 21 project of KREST (102-071-606), Center for Space-Time Molecular Dynamics (R11-2007-012-01002-0), and KISTI supercomputing center (KSC-2007-S00-1027).

## References and Notes

- (1) Leutwyler, S.; Bosiger, J. *Chem. Rev.* **1990**, *90*, 489-507.
- (2) Leist, R.; Frey, J. A.; Ottiger, P.; Frey, H. M.; Leutwyler, S.; Bachorz, R. A.; Klopffer, W. *Angew. Chem., Int. Ed.* **2007**, *46*, 7449-7452.
- (3) Trnka, T. M.; Grubbs, R. H. *Acc. Chem. Res.* **2001**, *34*, 18-29.
- (4) Kaye, S. S.; Long, J. R. *J. Am. Chem. Soc.* **2008**, *130*, 806-807.
- (5) Hu, X.; Trudeau, M.; Antonelli, D. M. *Chem. Mater.* **2007**, *19*, 1388-1395.
- (6) Choi, K.-W.; Kim, S. K.; Ahn, D.-S.; Lee, S. *J. Phys. Chem. A* **2004**, *108*, 11292-11295.
- (7) Choi, K.-W.; Choi, S.; Baek, S. J.; Kim, S. K. *J. Chem. Phys.* **2007**, *126*, 034308.
- (8) Ketkov, S. Y.; Selzle, H. L.; Cloke, F. G. N. *Angew. Chem. Int. Ed.* **2007**, *46*, 7072-7074.
- (9) Sohnlein, B. R.; Yang, D. S. *J. Chem. Phys.* **2006**, *124*, 134305.
- (10) Pribble, R. N.; Zwier, T. S. *Science* **1994**, *265*, 75-79.
- (11) Weber, T.; Neusser, H. J. *J. Chem. Phys.* **1991**, *94*, 7689-7699.
- (12) Fried, L. E.; Mukamel, S. *J. Chem. Phys.* **1992**, *96*, 116-135.
- (13) Philpott, M. R.; Kawazoe, Y. *J. Phys. Chem. A* **2008**, *112*, 2034-2042.
- (14) Sahnoum, R.; Mijoule, C. *J. Phys. Chem. A* **2001**, *105*, 6176-6181.
- (15) Rayon, V. M.; Frenking, G. *Organometallics* **2003**, *22*, 3304-3308.
- (16) Frisch, M. J.; Trucks, G. W.; Schlegel, H. B.; Scuseria, G. E.; Robb, M. A.; Cheeseman, J. R.; Montgomery, J. A., Jr.; Vreven, T.; Kudin, K. N.; Burant, J. C.; Millam, J. M.; Iyengar, S. S.; Tomasi, J.; Barone, V.; Mennucci, B.; Cossi, M.; Scalmani, G.; Rega, N.; Petersson, G. A.; Nakatsuji, H.; Hada, M.; Ehara, M.; Toyota, K.; Fukuda, R.; Hasegawa, J.; Ishida, M.; Nakajima, T.; Honda, Y.; Kitao, O.; Nakai, H.; Klene, M.; Li, X.; Knox, J. E.; Hratchian, H. P.; Cross, J. B.; Bakken, V.; Adamo, C.; Jaramillo, J.; Gomperts, R.; Stratmann, R. E.; Yazyev, O.; Austin, A. J.; Cammi, R.; Pomelli, C.; Ochterski, J. W.; Ayala, P. Y.; Morokuma, K.; Voth, G. A.; Salvador, P.; Dannenberg, J. J.; Zakrzewski, V. G.; Dapprich, S.; Daniels, A. D.; Strain, M. C.; Farkas, O.; Malick, D. K.; Rabuck, A. D.; Raghavachari, K.; Foresman, J. B.; Ortiz, J. V.; Cui, Q.; Baboul, A. G.; Clifford, S.; Cioslowski, J.; Stefanov, B. B.; Liu, G.; Liashenko, A.; Piskorz, P.; Komaromi, I.; Martin, R. L.; Fox, D. J.; Keith, T.; Al-Laham, M. A.; Peng, C. Y.; Nanayakkara, A.; Challacombe, M.; Gill, P. M. W.; Johnson, B.; Chen, W.; Wong, M. W.; Gonzalez, C.; Pople, J. A. *Gaussian 03*, revision C.02; Gaussian, Inc.: Wallingford, CT, 2004.
- (17) Hurley, M. M.; Pacios, L. F.; Christiansen, P. A.; Ross, R. B.; Ernler, W. C. *J. Chem. Phys.* **1986**, *84*, 6840.